arXiv:1411.3994v1 [astro-ph.HE] 14 Nov 2014

Coordinated Observations with Pulsar Timing Arrays and ISS-Lobster

Jeremy D. Schnittman

NASA Goddard Space Flight Center
Greenbelt, MD 20771

jeremy.schnittman@nasa.gov

ABSTRACT

Supermassive black hole binaries are the strongest gravitational wave sources in the universe. The systems most likely to be observed with pulsar timing arrays (PTAs) will have particularly high masses ($\gtrsim 10^9 M_\odot$), long periods ($T_{\rm orb} \gtrsim 1$ yr), and be in the local universe ($z \lesssim 1$). These features are also the most favorable for bright electromagnetic counterparts, which should be easily observable with existing ground- and space-based telescopes. Wide-field X-ray observatories such as ISS-Lobster will provide independent candidates that can be used to lower the threshold for PTA detections of resolvable binary sources. The primary challenge lies in correctly identifying and characterizing binary sources with long orbital periods, as opposed to "normal" active galactic nuclei (AGN) hosting single black holes. Here too ISS-Lobster will provide valuable new understanding into the wide range of behaviors seen in AGN by vastly expanding our sample of X-ray light curves from accreting supermassive black holes.

Subject headings: black hole physics – accretion disks – X-rays:binaries

1. EXECUTIVE SUMMARY

We present here an overview of coordinated electromagnetic (EM) and gravitational-wave (GW) observations of supermassive black holes binaries (SMBHBs) with the proposed ISS-Lobster all-sky soft X-ray imager and the Pulsar Timing Array (PTA) gravitational wave observatory. The feasibility of such a program depends on two major unknowns: the rate of SMBHB mergers in the local Universe, and the nature of associated EM signatures to such events.

To estimate the merger rates, we combine two relatively well-constrained observations: the galaxy merger rate at $z \lesssim 1$ and the SMBH mass function over the same time span. The

former comes from a variety of techniques, all of which seem to agree within a factor of order unity. We adopt the rates given by Lotz et al. (2011), which come from counting merger fractions in deep HST surveys, combined with theoretical/computational estimates for the amount of time a system will actually appear to be merging morphologically. The SMBH mass distribution function comes from X-ray surveys of AGN, combined with independent estimates of their typical Eddington-scaled accretion rates and duty cycles (Ueda et al. 2003; Merloni 2004).

Combined, we find merger rates of $R \sim 3\times10^{-4}$ Mpc^{-3} Gyr^{-1} for $M \approx 10^8 M_\odot$ and $R \sim 3\times10^{-5}$ Mpc^{-3} Gyr^{-1} for $M \approx 10^9 M_\odot$. For close binary systems, where the orbital evolution is governed by gravitational radiation, the amount of time spent at a given separation a is proportional to $a^4 \propto T_{\rm orb}^{8/3}$. For SMBHBs with $T_{\rm orb} \sim 1$ year (typical for PTA sources), the time-to-merger is still on the order of Myrs. This ensures that, while the merger *rates* are very small, the merger *fraction* can be much larger.

Out to redshift $z = 1$, we expect $N \approx 2 \times 10^5$ PTA sources with $M \sim 10^8 M_\odot$ and $N \approx 400$ for $M \sim 10^9 M_\odot$, which combine to give a characteristic GW strain amplitude of $h_c \sim 10^{-15}$. A simple rule of thumb for PTA strain sensitivity is $h \approx \delta t / T_{\rm obs}$, where δt is the accuracy of the pulsar timing residual measurement, and $T_{\rm obs}$ is the length of the observation. So to detect the expected stochastic signal at $f \sim (1\ {\rm yr})^{-1}$, a timing accuracy of $\sim$ 30ns would be required. From the population of thousands of unresolved SMBHBs, there is a small chance ($\sim$ few %) that one system will be particularly massive or nearby so that its GW signal rises above the background and can be individually resolved with PTA alone.

To estimate the EM signature of a merging SMBHB, we focus on theoretical models of circumbinary accretion disks. One generic feature of such a disk is the formation of hot spots near the inner edge of the disk, regions of large over-densities and emissivity. This disk flux can get upscattered into the soft X-ray band via inverse-Compton processes in the surrounding hot corona. Another common feature is the near-ballistic streams of gas flowing from the inner edge of the circumbinary disk, across a low-density gap, and colliding with the individual accretion disks found around each black hole. The X-ray emission from both these processes is expected to be modulated in time at roughly the orbital period, with a total flux proportional to the Eddington luminosity. For PTA-resolvable systems at distances of $\sim$ 100 Mpc, the X-ray flux from the disk+corona alone would almost certainly be observable by ISS-Lobster with high signal-to-noise.

Yet even at greater distances where the GW signal alone might not be resolvable, ISS-Lobster should still be able to detect the modulated X-ray signal. If we could measure its period and sky location with high precision, this information could be used to aid in the PTA

data analysis, potentially turning an unresolved source into a resolved source. If the existence of an EM counterpart can separate out the stochastic background, PTA timing noise of ~ 30 ns should be good enough to detect massive binaries out to ~ 350 Mpc, *giving a significant chance ($\approx 40\%$) of identifying a resolved PTA source with total mass $M \approx 10^9 M_\odot$*. Due to its relative proximity, high luminosity, and long lifetime, such a SMBHB candidate would be an excellent target for a wide variety of multi-wavelength follow-up observations.

Out to distances of $D_L \approx 1$ Gpc, ISS-Lobster might identify as many as 10 massive binaries with periodic light curves, but essentially no chance to resolve their GW signal with the current PTA sensitivity. By comparing ISS-Lobster source number counts with the slope and amplitude of the stochastic GW signal, we may be able to infer something about the physical mechanisms (i.e., massive gas disks, three-body scattering, gravitation radiation, etc.) driving SMBHB evolution in the PTA regime.

Lastly, even in the absence of unambiguous detections of SMBHBs, ISS-Lobster will provide long-duration X-ray light curves of roughly 400 AGN sampled with weekly cadence. Such a data set will be essential for understanding the broad range of normal AGN activity, and thus provide a control group against which to compare binary candidates.

2. PULSAR TIMING ARRAYS

Much like EM astronomy, gravitational wave astronomy has historically been divided into two complementary approaches, ground-based (e.g., LIGO/Virgo) and space-based (LISA), roughly corresponding to stellar-mass and super-massive black hole sources, respectively. In recent years, a hybrid approach has emerged, that of pulsar timing arrays. PTAs used ground-based radio telescopes to measure the effect of GWs on the propagation of radio pulses from millisecond pulsars distributed throughout the galaxy. The GWs impart a characteristic delay on the arrival times of the pulses at Earth. By comparing the arrival times with an underlying model for the pulsar/Earth/Sun system, a "residual" is measured. The timing residuals from different pulsars are correlated in a very well-defined way, providing additional angular information about any potential underlying GW signal [Hellings & Downs (1983), see Hobbs et al. (2010) for a review of the current instruments and future sensitivity projections].

The predominant sources for PTAs are supermassive black hole binaries at cosmological distances. These sources can generally be divided into two categories: stochastic and resolved. This is primarily a data analysis, rather than astrophysical, distinction. By most estimates, the stochastic population is more likely to be detected by first-generation PTAs.

The resolved population—if detected—would simply be the brightest subset of the total population of SMBHBs throughout the universe. In practice, they are more massive, relatively closer, and at higher GW frequencies (and thus closer to merger) than the average SMBHB. Table 1 shows the typical order-of-magnitude properties of systems in these two source classes.

Table 1: Typical properties of SMBHBs making up the stochastic and resolved populations of PTA sources.

	stochastic	resolved
$M_{\rm BH}$ ($M_\odot$)	10^8	10^9
$f_{\rm GW}$ (Hz)	10^{-8}	10^{-7}
$q = M_2/M_1$	0.1-1	1
D_L (Gpc)	10	0.1
GW strain h_c	10^{-19}	10^{-14}

Since we expect any gas-powered electromagnetic (EM) counterparts to be limited to roughly Eddington luminosities, both these features (high mass and small distance) work in our favor to make the resolved population of PTA sources bright enough to see easily with EM telescopes. Furthermore, working under the assumption that the dynamics of galaxy mergers promote more gas flow into the central regions, we expect SMBHBs to have higher average accretion rates relative to isolated AGN (Treister et al. 2012). While the most massive BHs will likely reside in massive, gas-poor elliptical galaxies, this clearly does not preclude the possibility of quasar activity (Kirhakos et al. 1999).

3. EM MECHANISMS

An exhaustive review of potential electromagnetic signatures of SMBH mergers is provided in Schnittman (2013) [for recent work on the subject, and particularly for PTA-relevant sources, see Tanaka et al. (2012); Sesana et al. (2012); Tanaka & Haiman (2013); Burke-Spolaor (2013); D'Orazio et al. (2013); Farris et al. (2014)]. Figure 1 (reproduced from Schnittman 2013) shows a sample of the mechanisms that could produce an EM signature. They can be roughly divided into direct and indirect evidence for mergers, or alternatively, "counterparts" and "signatures." In this discussion we will use the term counterpart to refer to an EM signal that is detected (or at least detectable) along with a concurrent GW signal. A signature is either a direct or indirect EM signal that has no associated GW

detection (we do not consider the GW stochastic background to be "associated" with any specific EM signal).

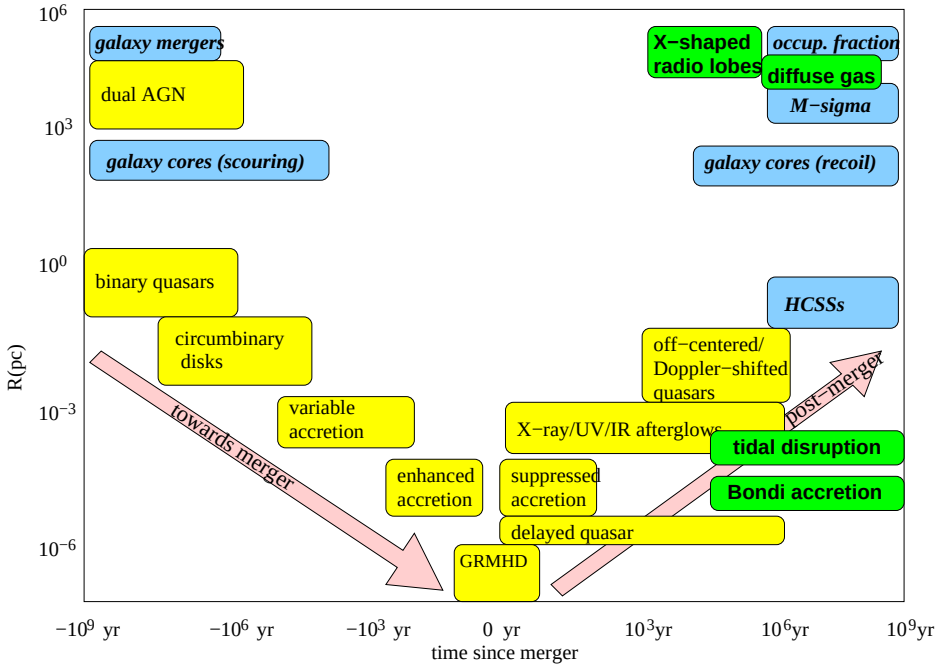

Fig. 1.— Selection of potential EM sources, sorted by timescale, typical size of emission region, and physical mechanism (blue/*italic* = stellar; yellow/Times-Roman = accretion disk; green/**bold** = diffuse gas/miscellaneous). The evolution of the merger proceeds from the upper-left through the lower-center, to the upper-right.

The axes in Figure 1 are distance from merger vs time before/after merger. The sources evolve from the upper-left through the lower-center, to the upper-right of the figure. For the most part, EM counterparts come from the lower-left/lower-center regions where GW emission is strongest and most likely to be detected with PTA observations. These sources all rely on the presence of relatively dense, cool gas in the form of accretion flows around the two black holes.

Thus the study of EM counterparts to SMBHB GW sources is fundamentally one of understanding the behavior of circumbinary accretion disks. More specifically, we would like to understand how the behavior of circumbinary disks differs from that of active galactic nuclei (AGN) driven by single black holes. We have decades of observations of AGN across many wavelengths, with ever-improving spatial, spectral, and temporal resolution. As evidenced by the multi-dimensional zoological classification schemes (e.g., Antonucci 2011)

needed to describe the variety of AGN observations, it is notoriously hard to say exactly what a "normal" AGN looks like.

Most 1D analytic models of circumbinary disks suggest that the additional outward torques that the binary imposes on the disk will arrest significant accretion, and thus EM luminosity, leaving an evacuated region around the two black holes (Pringle 1991; Milosavljevic & Phinney 2005). However, virtually all 2D and 3D simulations of circumbinary disks show significant accretion across the inner gap, generally along two gas streams as seen if Figure 2. Other generic features include a low-density region with radius $R_{\rm in} \sim 2a$, with a the semi-major axis of the binary, eccentric orbits for the disk, and spiral density waves excited in the inner disk. These density waves in turn impart a gravitational torque on the binary and cause it to shrink [however, recent work suggests that *retrograde* circumbinary disks may show very different behavior and evolution (Nixon et al. 2011; Roedig & Sesana 2014; Bankert et al. 2014; Schnittman & Krolik 2014)].

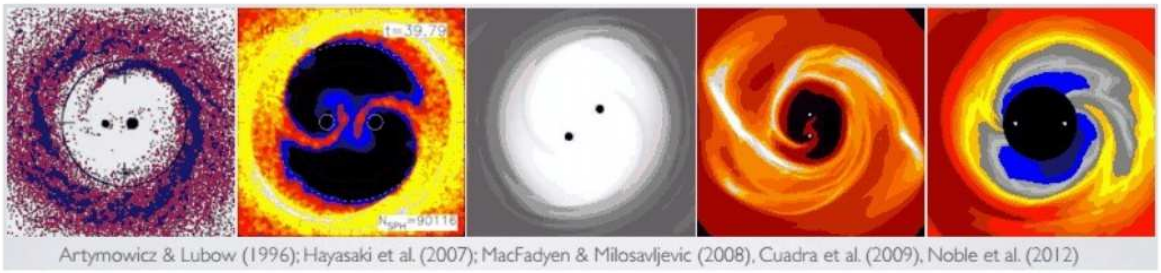

Fig. 2.— Snapshots from a variety of 2D and 3D simulations of circumbinary disks, taken from Artymowicz & Lubow (1996); Hayasaki et al. (2007); MacFadyen & Milosavljevic (2008); Cuadra et al. (2009); Noble et al. (2012).

In addition to these features, recent grid-based 3D magneto-hydrodynamic (MHD) simulations by Shi et al. (2012); Noble et al. (2012) show the presence of a strong $m = 1$ density perturbation at radius $R \approx 2.5a$, shown in Figure 3. The beat frequency between the lump's orbital period and that of the binary leads to a strong modulation in the disk luminosity at frequency $\Omega \approx 1.5\Omega_{\rm bin}$, corresponding to each of the binary members gravitationally exciting the region of over-density, in turn leading to a raised level of local emission. In addition to the variability in the total luminosity, there should also be a variation in the measured flux as seen by an inclined observer, due to the Doppler shifting of the hot spot moving towards and away from the observer, with frequency corresponding to the Keplerian frequency of the orbiting lump $\Omega_{\rm lump} \approx 0.25\Omega_{\rm bin}$ (Noble et al. 2012).

For the typical masses and densities for AGN disks, the disk should be optically thick

and emitting primarily in the optical/UV. In almost every AGN observed in the X-ray, there appears to be a hot, tenuous corona surrounding the accretion disk, leading to inverse-Compton scattering of the thermal seed photons up to ~ 100 keV with luminosity of roughly 10% of the total bolometric luminosity. So even if the lump is fundamentally a disk feature, it should still show up in the X-ray light curves due to the local inverse-Compton emission immediately above the lump. Noble et al. (2012) find that the global luminosity variability has an amplitude of $\sim 5-10\%$. For an observer at inclination i, the Doppler-shifted intensity will scale roughly like $(\delta\rho/\rho)(1+\sin i\, v/c)^3$. For a circular orbit with binary separation of a and canonical observer with $i = 60°$, this corresponds to $\delta I/I \sim 2a^{-1/2}$.

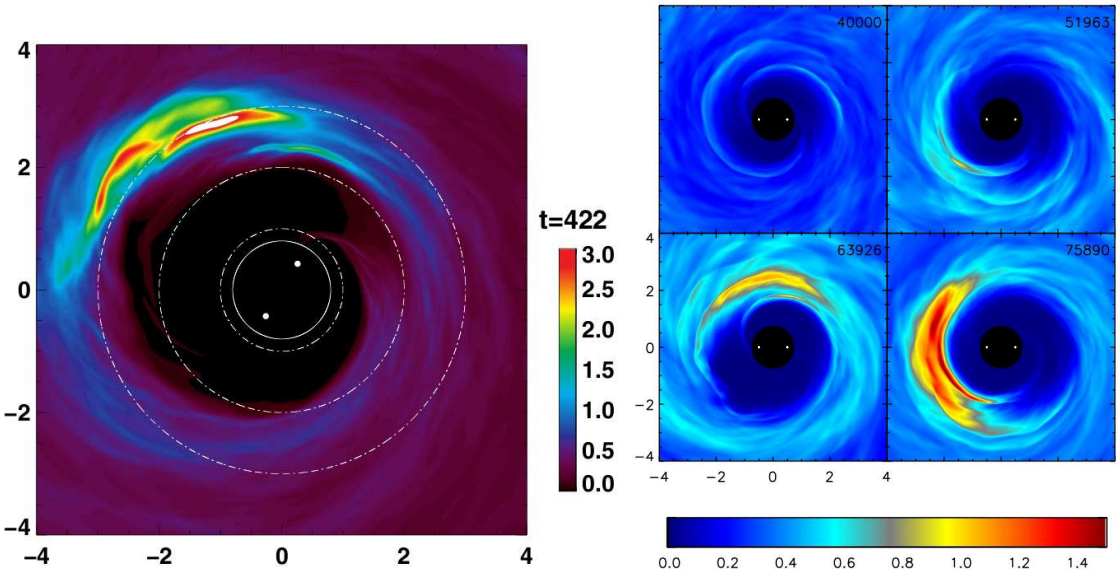

Fig. 3.— Surface density from two different MHD simulations of circumbinary disks. *left*: Shi et al. (2012); *right*: Noble et al. (2012). In both cases, over-dense "lumps" are formed near the inner edge of the disk.

What binary separations might we expect for the PTA sources? From Kepler's first law, we can write

$$a = 100 r_g \left(\frac{T_{\rm orb}}{1\ {\rm yr}}\right)^{2/3} \left(\frac{M}{10^9 M_\odot}\right)^{-2/3}, \qquad (1)$$

where M is the total mass of the binary and $r_g = GM/c^2$ is the gravitational radius, the standard unit of length in the system. From this expression, we see that when the binary orbital period is one year, the system is already entering the relativistic regime with $v/c \sim 0.1$, or an X-ray modulation of $10-20\%$.

Roedig et al. (2014) recently explored two specific spectral signatures of a circumbinary

disk: a low-energy notch in the spectrum and a high-energy excess, shown in Figure 4. Both signatures assume the existence of individual accretion disks around each black hole, something that is typically very difficult to resolve numerically in simulations. Assuming these "mini-disks" do exist, they will likely extend out to some fraction of the semimajor axis a, inside of which they should behave like normal disks, with gravitational binding energy being released through gas accretion via the magneto-rotational instability. Similarly, well outside of the gap region the circumbinary disk should behave like a regular accretion disk. Since the temperature of a classical disk scales like $R^{-3/4}$, each radius contributes to a different part of the continuum spectrum. By removing the gas from the gap region between the inner mini-disks and the outer circumbinary disk, a corresponding notch will be removed from the spectrum. This is shown in Figure 4, reproduced from Roedig et al. (2014), where T_0 is the temperature of the inner edge of the circumbinary disk. The exact location and shape of this notch feature will depend on the binary separation, accretion rate, black hole masses, and mass ratio.

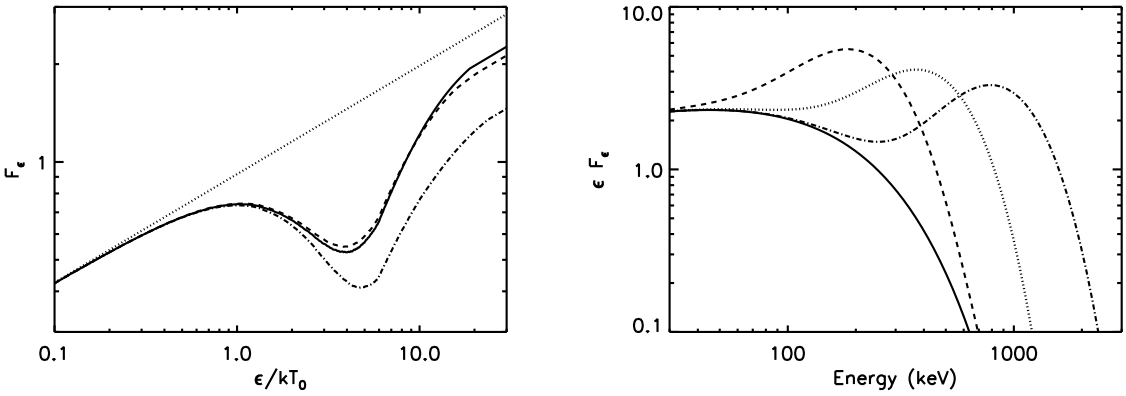

Fig. 4.— Spectra of circumbinary disk AGN, with the left figure showing the missing continuum emission from the gap (scaled to the thermal temperature T_0 at the inner edge of the disk), and the right figure showing the high-energy emission caused by streams shocking on the inner accretion "mini-disk." The different curves in each plot represent a range of reasonable model parameters, along with the coronal emission expected from a normal AGN (*right, solid curve*). [reproduced from Roedig et al. (2014)]

Also shown in the right panel of Figure 4 is the high-energy emission expected from the gas streaming from the outer disk into the inner disks and forming high-temperature shocks. With stream velocities comparable to the binary orbital velocity, post-shock temperatures will be of the order $kT \sim GM/a$, with fiducial values of $\sim$ 200 keV for separation of $a \sim 10^3 r_g$. This hot gas will generally cool rapidly through pair production and inverse-

Compton scattering of seed photons from the mini-disks, producing a modulated hard X-ray signal with luminosity proportional to mass flow across the gap. For eccentric disks (or binaries), modulations of the accretion rate on the order of 10% or higher should be common (MacFadyen & Milosavljevic 2008; Shi et al. 2012; Noble et al. 2012).

In the shock-stream model, the mini-disks around each black hole should also power a corona, and thus contribute to the X-ray flux. Since the majority of potential energy is extracted in the inner-most region of the disk, it is in fact quite likely that the mini-disks dominate the total X-ray flux from the system. In that scenario, the hard X-ray flux ($\gtrsim 100$ keV) will come predominately from the shock points, while the softer X-rays ($\sim 1-10$ keV) will come from inverse-Compton scattering of the mini-disk photons off of mini-coronas.

If the mini-disks do in fact dominate the emission, then the chance of detection with ISS-Lobster will be greater, but the variable fraction of the signal may be smaller, depending on the inflow timescales of the mini-disks. If the inflow time is long compared to the orbital period, then the mini-disks will absorb the variable accretion across the gap and damp out any modulation in the light curve. However, if the inflow time is comparable to the orbital period, the mini-disk emission should vary with the same period and amplitude as the accretion streams. In both cases, there should still be relativistic Doppler beaming of the mini-disk flux, again leading to variability amplitudes on the $\sim 10-20\%$ level.

It should be noted that all of these emission mechanisms are nearly isotropic, further enabling joint GW-EM observations. This is in marked contrast to the leading candidates for LIGO EM counterparts, the highly relativistic, beamed jets from gamma-ray bursts (GRBs). While kilonovae counterparts would be largely isotropic, they would also have significantly lower flux, making them much harder to detect with EM observations (Metzger & Berger 2012). Additionally, because the PTA GW sources are continuous and long-lived, signal-to-noise will grow steadily in time along with the X-ray light curves.

4. RATES

Traditionally, event rates for space-based gravitational wave detectors like LISA have been based on large-scale N-body cosmological simulations tracking the mergers of galaxies and their central SMBHs from the early Universe through today. This is necessary because many of the sources will likely be at high redshift $z \gtrsim 5-10$ where there are no solid observational constraints for the event rates (Sesana et al. 2005, 2007). While this approach should also work in principle for PTA sources (Sesana et al. 2008), because they tend to be much closer (see Table 1), we do not need to rely on purely theoretical calculations of their

rates.

EM observations of galaxy merger rates at $z \lesssim 1.5$ should be sufficient estimates of SMBH merger rates relevant to PTA observations (and probably more accurate than N-body simulations). Lotz et al. (2011) find the major merger rate ($1/4 < M_2/M_1 < 1$) this range to be ~ 0.1 Gyr^{-1} per galaxy, and the minor merger rate ($1/10 < M_2/M_1 < 1/4$) to be roughly three times that. Combined with the black hole mass function derived from X-ray surveys such as Ueda et al. (2003) and Merloni (2004), we get merger rates of $R \sim 3 \times 10^{-4}$ Mpc^{-3} Gyr^{-1} for $M \approx 10^8 M_\odot$ and $R \sim 3 \times 10^{-5}$ Mpc^{-3} Gyr^{-1} for $M \approx 10^9 M_\odot$. This "back-of-the-envelope" approach agrees reasonably well with a more detailed analysis by Sesana (2013a).

To estimate the number of sources in the sky at any one time, one needs to multiply the rate times the time that the source spends in that phase. For SMBHBs in the GW-dominated phase of evolution, the characteristic time spent at a binary separation a is (Peters 1964)

$$t_{\rm GW} = \frac{a}{\dot{a}} = \frac{5}{64} \frac{c^5}{G^3 M^3} \frac{(1+q)^2}{q} a^4 \,, \tag{2}$$

where M is the total mass and q is the mass ratio. Combining with equation (1), and for a fiducial mass ratio of $q = 1/3$, the timescale $t_{\rm GW}$ spent with GW period around 1 yr is $\sim 5 \times 10^6$ yr for $M = 10^8 M_\odot$ and $\sim 10^5$ yr for $10^9 M_\odot$. This corresponds to a total number of PTA sources out to $z = 1$ of $N(M > 10^8 M_\odot) \approx 2 \times 10^5$ and $N(M > 10^9 M_\odot) \approx 400$.

5. OBSERVABILITY

The characteristic (i.e., averaged over sky location and source orientation) strain amplitude from a binary source at luminosity distance D_L and observed frequency $f_{\rm GW} = 2T_{\rm orb}^{-1}(1+z)^{-1}$ is given by

$$h_c = \frac{G\mathcal{M}}{c^2 D_L} \left(\frac{G\pi f_{\rm GW} \mathcal{M}}{c^3} \right)^{2/3} \,, \tag{3}$$

where the chirp mass is defined as $\mathcal{M} = (M_1 M_2)^{3/5} M^{-1/5} = q^{3/5}(1+q)^{-6/5} M$. At a redshift of $z = 1$, this gives a characteristic strain of

$$h_c(z=1) \approx 5 \times 10^{-17} \frac{q}{(1+q)^2} \left(\frac{M}{10^9 M_\odot} \right)^{5/3} \left(\frac{T_{\rm orb}}{1 \text{ yr}} \right)^{-2/3} \,. \tag{4}$$

Again using $q \sim 1/3$, and summing over the incoherent populations of binaries out to $z = 1$, we find

$$h_c(M > 10^{8.5} M_\odot) \sim 3 \times 10^{-16} \tag{5}$$

and

$$h_c(M < 10^{8.5} M_\odot) \sim 1.5 \times 10^{-16} \,. \tag{6}$$

These very rough estimates are actually in quite close agreement with those predicted by Sesana (2013a,b), using Monte Carlo realizations of the Universe, based on observed galaxy merger rates and black hole distribution function out to $z \sim 1.5$. Furthermore, this stochastic signal should be within reach of reasonable PTA sensitivity estimates within the next 5-10 years (Sesana 2013a,b).

For a single source to rise up above the background, let us estimate that its strain should be roughly twice that of the stochastic signal [However, careful data analysis techniques such as matched filtering may allow for the identification of an individual source with signal strength comparable to the background, thereby increasing the chance of detection with time. (A. Sesana, private communication)]. For $M = 10^9 M_\odot$, this corresponds to a distance of $D_L \lesssim 100$ Mpc, or a co-moving volume 3×10^4 times smaller than that occupied by the stochastic population. The expected number of binaries in this volume with orbital periods of ~ 1 year is only ~ 0.01, so the chance of detecting a resolved GW source with PTA alone is maybe a few percent in the optimistic limit.

We may get lucky with a particularly massive binary with $M > 10^{10} M_\odot$, but the black hole distribution function at the high end of the mass range is poorly known, so it is very difficult to make even rough estimates. Similarly, pushing to higher frequencies and more equal mass ratios will increase the distance at which point the sources are resolved, but also move into the regime where PTA is less sensitive (the observable strain scales like $h \propto f$ at high frequency).

On the other hand, by extending to lower frequencies (i.e., longer observations), the number of sources could be increased by a factor of $(a/a_{1\ \mathrm{yr}})^4 = (T_{\mathrm{orb}}/1\ \mathrm{yr})^{8/3}$. Of course, more sources will make the stochastic signal stronger, making it more difficult to resolve individual sources. At the same time, by going to very long-period orbits, there is a very good chance that the binary separation will move out of the purely GW-driven evolution and begin to probe additional larger-scale astrophysical mechanisms such as disk-driven migration and three-body relaxation with surrounding stars (Begelman et al. 1980; Kocsis & Sesana 2011; Sesana 2013b; Ravi et al. 2014).

What about electromagnetic observability? Let us first consider the less uncertain model of emission from the circumbinary disk. In normal accretion disks, the primary source of EM power is the conversion of gravitational potential energy into turbulent magnetic stress within the disk body Balbus & Hawley (1991). This is in turn converted to both thermal disk radiation and high-energy X-rays via inverse-Compton scattering in the corona (Noble et al. 2011; Schnittman et al. 2013). The radiative efficiency of such a disk is roughly $1 - E_{\mathrm{ISCO}}$,

where $E_{\rm ISCO}$ is the specific energy of the gas at the inner edge of the accretion disk. In the Newtonian limit, $E_{\rm ISCO} = c^2/(2r_{\rm ISCO})$ with $r_{\rm ISCO}$ measured in gravitational radii. For a circumbinary disk with inner edge $r_{\rm in} = 2a$, the radiative efficiency is reduced by a factor of $r_{\rm ISCO}/(2a)$.

If the gas is supplied at large radius at $\dot{m}$ times the Eddington accretion rate, the EM luminosity of the disk alone will be

$$L_{\rm disk} = \dot{m} L_{\rm Edd} \left(\frac{r_{\rm isco}}{2a}\right) \approx 2 \times 10^{45}\, \dot{m} \left(\frac{M}{10^9 M_\odot}\right)^{5/3} \left(\frac{T_{\rm orb}}{1\ {\rm yr}}\right)^{-2/3}\ {\rm erg/s}\,. \tag{7}$$

Typical AGN have X-ray fractions of the total bolometric luminosity of $f_x \sim 0.1$ in the ISS-Lobster band. For GW-resolvable sources at $D_L = 100$ Mpc, the X-ray flux will be

$$F_x = \dot{m} \frac{f_x}{0.1} 10^{-11}\, {\rm erg/s/cm^2}\,, \tag{8}$$

with a modulation of $\sim 20\%$ on timescales of the orbital period.

For the shocked streams discussed above, f_x would likely be significantly smaller, since most of the associated emission is limited to energies above 10 keV. Including the emission from the mini-disks/coronae will increase the X-ray flux by another factor of $\sim (a/r_{\rm ISCO})$, with comparable levels of variability. This would mean equation (8) could hold for sources as far as $D_L \approx 1$ Gpc! In this volume, there could be as many as ~ 10 SMBHBs in the PTA band with total mass greater than $10^9 M_\odot$.

ISS-Lobster is expected to reach flux levels of 10^{-11} erg/s/cm^2 for the entire sky scan each day. This means that any source that is potentially resolvable with PTA observations should be easily observable with ISS-Lobster, as long as it is accreting a significant amount of gas. Large scale gas flows and accretion have long been predicted as generic features of galaxy mergers, and there is mounting observational evidence that there is in fact a strong correlation between galaxy mergers and AGN activity (Koss et al. 2012). Not only do galaxy mergers drive gas inflow, but gas inflow in turn drives black hole mergers (Cuadra et al. 2009), further increasing the likelihood that SMBHBs will be formed and observed in the presence of circumbinary disks with relatively high values of $\dot{m}$.

On a weekly timescale, ISS-Lobster should be able to sample roughly 400 AGN in the sky with fluxes greater than $\approx 2 \times 10^{-12}$ erg/s/cm^2 (Hasinger et al. 2005). From the event rates calculated above, we estimate there is a moderate chance that one of these objects is in fact a SMBHB in the PTA band, but too far away to resolve from the GW signal alone. However, with the sky location and precise orbital period provided by ISS-Lobster, it is quite possible that the GW signal could be picked out from the stochastic background. If in

fact we could separate the individual signal from the background, equation (3) suggests that current PTA detectors should be sensitive out to $D_L \approx 350$ Mpc for $M = 10^9 M_\odot$. Within this range, there is $\approx 40\%$ chance of such a SMBHB existing. The range for $M = 10^8 M_\odot$ is only $D_L \approx 6$ Mpc, giving almost no chance of resolving a PTA source (which is why they are in the stochastic category in the first place!).

For the canonical stochastic PTA sources, the X-ray flux would be on the order of $\sim 10^{-15}$ erg/s/cm^2. While far too faint for ISS-Lobster, these objects would certainly show up in the Chandra deep field surveys, but identification as periodically variable sources would be nearly impossible.

6. DISCUSSION

We must end this discussion the same way it began, with a clear disclaimer: the rates and properties of the SMBHB sources discussed above are intentionally very rough approximations, accurate to an order of magnitude at best. We simply do not believe greater precision is justified or even particularly helpful at this stage in the field. Yet even these rough theoretical estimates are more than enough to justify intense and comprehensive observational campaigns, which will hopefully yield actual detections, or at the very least, more reliable limits.

From a variety of independent methods (N-body cosmological simulations, deep field HST and ground-based surveys, local Universe AGN surveys), the merger rate of galaxies and their central black holes appears to be roughly one major—and a few minor—mergers per galaxy per Hubble time. This implies several hundred (thousand) SMBHBs with total masses $\sim 10^9 M_\odot$ ($10^8 M_\odot$), orbital periods of roughly one year, and within the volume out to $z = 1$. Combined, these thousands of sources contribute to a stochastic background with characteristic strain amplitude of $h_c \lesssim 10^{-15}$. While typical isolated SMBHs have relatively low duty cycles, it is believed that the galactic merger process will make it much more likely that the SMBHB sources are accreting gas at nearly the Eddington rate, leading to particularly bright and variable X-ray sources.

There is a small chance that a few SMBHB sources might lie sufficiently close or be sufficiently massive such that their GW signal rises above the stochastic background and can be individually resolved with PTA observations. If these systems also have circumbinary accretion disks, they will almost certainly be detectable with high signal-to-noise with ISS-Lobster. Such a combined EM-GW signal would greatly raise the significance of both measurements, and undoubtedly lead to a massive multi-wavelength targeted observation

campaign.

There is a larger number of sources that should be within the detection limits of ISS-Lobster, but only resolvable with PTA if the sky position and frequency are known *a priori*. Thus the ISS-Lobster–PTA synergy has great potential to significantly enhance both science programs. To a certain extent, this is the converse of the analogous LIGO-GRB connection, where many off-axis GW sources will be seen by LIGO with high SNR, but go undetected in the EM spectrum.

Even for the unresolvable sources, there is much to be learned from coordinated ISS-Lobster–PTA science. In particular, the high-cadence observations of roughly 400 AGN in the X-ray band will expand our sample of long-baseline AGN light curves by nearly two orders of magnitude. Time-domain observations of a few of the brightest AGN have shown us that there is a very wide range of variability behavior from single accreting black hole systems. Thus it is imperative to fully explore the range of "normal" AGN before we have a convincing chance to identify a given source as a binary from the light curve alone. ISS-Lobster will do exactly this, and also provide promising targets for deeper, targeted multi-wavelength observing campaigns of the most interesting variable sources, much like has been done for BAT-selected AGN studies such as Koss et al. (2012).

Similarly, the amplitude and slope of the unresolved stochastic GW background will provide important limits on the evolution of SMBHB systems. The balance of gas-driven migration, stellar scattering, and gravitational radiation losses all combine to give a complex picture of the evolution of merging black holes and their environments (Ravi et al. 2014). By including population information from ISS-Lobster (as well as complementary surveys like the Chandra deep field and XMM-Newton COSMOS field), we will have constraints to theoretical models of binary evolution. For example, if we detect many bright X-ray sources, but a relatively low GW signal, it might indicate gas-driven evolution well beyond the conventional stage where the disk decouples from the binary (Milosavljevic & Phinney 2005). On the other hand, a flat GW spectrum, coupled with a lack of periodic X-ray sources, might suggest that high-eccentricity binaries are common and the gas disk decouples at an early stage (Schnittman & Krolik 2014).

Acknowledgments: We would like to thank Jordan Camp, Cole Miller, and Alberto Sesana for many useful comments. This work was supported in part by NASA grant ATP12-0139.

REFERENCES

Antonucci, R. 2011, arXiv:1101.0837

Artymowicz, P., & Lubow, S. H. 1996 *Astroph. J. Lett.* **467**, 77

Balbus, S. A., & Hawley, J. F. 1991, *Astroph. J.* **376**, 214

Bankert, J., Krolik, J. H., & Shi, J.-M. 2014, *Astroph. J.* submitted

Begelman, M. C., Blandford, R. D., & Rees, M. J. 1980 *Nature* **287**, 307

Burke-Spolaor, S. 2013, *Clas. Quant. Grav.* **30**, 224013

Cuadra J., Armitage P. J., Alexander, R. D., & and Begelman, M. C. 2009 *Mon. Not. Royal Astron. Soc.* **393** 1423

D'Orazio, D. J., Haiman, Z., & MacFadyen, A. 2013, *Mon. Not. Royal Astron. Soc.* **436**, 2997

Farris, B. D., Duffell, P., MacFadyen, A. I., & Haiman, Z. 2014, *Astroph. J.* **783**, 134

Hasinger, G., Miyaji, T., & Schmidt, M. 2005, *Astron. Astroph.* **441**, 417

Hayasaki, K., Mineshige, S., & Sudou, H. 2007, *Publ. Astron. Soc. Japan* **59**, 427

Hellings, R. W., & Downs, G. S. 1983, *Astroph. J. Lett.* **265**, L39

Hobbs, G., et al. 2010, *Clas. Quant. Grav.* **27**, 084013

Kirhakos, S., Bahcall, J. N., Schneider, D. P., & Kristian, J. 1999, *Astroph. J.* **520**, 67

Kocsis, B., & Sesana, A. 2011, *Mon. Not. Royal Astron. Soc.* **411**, 1467

Koss, M., et al. 2012, *Astroph. J. Lett.* **746**, 22

Lotz, J. M., Jonsson, P., Cox, T. J., Croton, D., Primack, J. R., Somerville, R. S., & Stewart, K. 2011, *Astroph. J.* **742**, 103

MacFadyen, A. I., & Milosavljevic, M. 2008, *Astroph. J.* **672** 83

Merloni, A. 2004, *Mon. Not. Royal Astron. Soc.* **353**, 1035

Metzger, B. D., & Berger, E. 2012, *Astroph. J.* **746**, 48

Milosavljevic, M., & Phinney, E. S. 2005 *Astroph. J. Lett.* **622**, 93

Nixon, C. J., Cossings, P. J., King, A. R., & Pringle, J. E. 2011, *Mon. Not. Royal Astron. Soc.* **412**, 1591

Noble, S. C., Krolik, J. H., Schnittman, J. S., & Hawley, J. F. 2011, *Astroph. J.* **743**, 115

Noble, S. C., Mundim, B. C., Nakano, H., Krolik, J. H., Campanelli, M., Zlochower, Y., & Yunes, N. 2012, *Astroph. J.* **755**, 51

Peters, P. C. 1964, Phys. Rev. **136**, 1224

Pringle, J. E. 1991, *Mon. Not. Royal Astron. Soc.* **248**, 754

Ravi, V., Wyithe, J. S. B., Shannon, R. M., Hobbs, G., & Manchester, R. N. 2014, *Mon. Not. Royal Astron. Soc.* **442**, 56

Roedic, C., & Sesana, A. 2014, *Mon. Not. Royal Astron. Soc.* **439**, 3476

Roedig, C., Krolik, J. H., & Miller, M. C. 2014, *Astroph. J.* , **785**, 115

Schnittman, J. D. 2013, *Clas. Quant. Grav.* **24**, 244007

Schnittman, J. D., Krolik, J. H., & Noble, S. C. 2013, *Astroph. J.* **769**, 156

Schnittman, J. D., & Krolik, J. H. 2014, *Astroph. J.* submitted

Sesana, A., Haardt, F., Madau, P., & Volonteri, M. 2005, *Astroph. J.* **623**, 23

Sesana, A., Volonteri, M., & Haardt, F. 2007, *Mon. Not. Royal Astron. Soc.* **377**, 1711

Sesana, A., Vecchio, A., & Colacino, C. N. 2008, *Mon. Not. Royal Astron. Soc.* **390**, 192

Sesana, A., Roedig, C., Reynolds, M. T., & Dotti, M. 2012, *Mon. Not. Royal Astron. Soc.* **420**, 860

Sesana, A. 2013a, *Mon. Not. Royal Astron. Soc.* **433**, L1

Sesana, A. 2013b, *Clas. Quant. Grav.* **30**, 244009

Shi, J.M., Krolik, J. H., Lubow, S. H., & Hawley, J. F. 2012, *Astroph. J.* **749**, 118

Tanaka, T., Menou, K., & Haiman, Z. 2012, *Mon. Not. Royal Astron. Soc.* **420**, 705

Tanaka, T., & Haiman, Z. 2013, *Clas. Quant. Grav.* **30**, 224012

Treister, E., Schawinski, K., Urry, C. M., & Simmons, B. D. 2012, *Astroph. J. Lett.* **758**, 39

Ueda, Y., Akiyama, M., Ohta, K., & Miyaji, T. 2003, *Astroph. J.* **598**, 886

This preprint was prepared with the AAS LaTeX macros v5.0.